

INVESTIGATION OF THERMAL BEHAVIOR AND FLUID MOTION IN DIRECT CURRENT MAGNETOHYDRODYNAMIC PUMPS

by

**Mehdi KIYASATFAR^{a*}, Nader POURMAHMOUD^a, Maqsood GOLZAN^b,
and Iraj MIRZAEI^a**

^a CFD Research Center, Mechanical Engineering Department, Urmia University,
Urmia, West Azerbaijan, Iran

^b Physics Department, Faculty of Science, Urmia University, Urmia, West Azerbaijan, Iran

Original scientific paper

DOI: 10.2298/TSCI110826089K

Motivated by increasingly being used magnetohydrodynamic micropumps for pumping biological and chemical specimens, this study presents a simplified magnetohydrodynamic flow model based upon steady-state, incompressible and fully developed laminar flow theory in rectangular channel to offer the characteristics of magnetohydrodynamic pumps for prediction of pumping performance in magnetohydrodynamic flow. The non-linear governing equations of motion and energy including viscous and Joule dissipation are solved numerically for velocity and temperature distributions. To aim this goal a finite difference approximation based code is developed and utilized. In addition, the effects of magnetic flux density, applied electric current and channel size on flow velocity field as well as thermal behavior are investigated in various working medium with different physical properties. The entropy generation rate is discussed also. The simulation results are in good agreement with experimental data from literature.

Key words: magnetohydrodynamic, micropumps, Lorentz forces, entropy generation

Introduction

Application of microfluidic devices has rapidly extended to a wide variety of fields in the last two decades. Microfluidic devices are used in various applications such as micropumps, reactors, mixers and pressure flow sensors. The micropumps, as an important actuator, are the basic sign of the development level of microfluidic systems. The magnetohydrodynamic (MHD) micropump is one of the important microfluidic systems that has no moving parts, generates continuous flow, and is very suitable to use in biomedical applications. The pumping source in MHD micropumps is the Lorentz force, which is produced as a result of an interaction between magnetic and electric fields.

Theoretical and experimental studies on DC and AC MHD devices have been investigated recently.

Lemoff *et al.* [1] and Lemoff and Lee [2] constructed a practical AC MHD pump in which the Lorentz force is used to propel an electrolytic solution along a microchannel etched in silicon. Experimental measurements were conducted on various concentrations of sodium chloride (NaCl) solutions to determine the maximum current allowed in the micro-channels before gas bubbles were observed. The experimental studies indicate that the electrolysis phenomenon was greatly reduced when the frequency of the applied current was sufficiently

* Corresponding author; e-mail: m.kiyasatfar@gmail.com

high. Jang and Lee [3] presented a DC micro-pump, and obtained the performance of the MHD micro-pump in single phase and using simple model. In addition to MHD pumping, the study of mixing systems and microfluidic networks using MHD pumping has been performed. Lemoff and Lee [4] used MHD forces to pump electrolytic solutions in microfluidic networks. Wang *et al.* [5] replicated a simplified MHD flow model based upon steady state, incompressible and fully developed two-dimensional laminar flow to take into account of the frictional effects on the channel side walls of the MHD pump. In their study, the Lorentz forces are converted into the hydrostatic pressure gradient in the momentum equation. To avoid gas bubbles, Homsy *et al.* [6] described the operation of DC MHD micro-pump with high current densities without gas bubbles inside of the pumping channel. Duwairi and Abdullah [7] presented a transient fully developed laminar flow and temperature distribution in a MHD micro pump. They numerically and analytically studied the effect of different important parameters, on the transient velocity and temperature. Ho [8] in his research, focused on the prediction of pumping performance in MHD flow. To aim this goal, an analytical model based on the steady state, incompressible and fully developed laminar flow theory was provided to analyze the flow characteristic with different scalar dimensions in duct channel.

The analysis of entropy generation, that was firstly formulated by Bejan [9, 10], has found a variety of applications such as the assessment of heat exchangers, two-phase flows, fuel cells and many others. Salas H., [11] studied an entropy generation analysis that was applied to the optimization of MHD flows to induction devices. Haddad *et al.* [12] investigated entropy generation due to laminar, incompressible forced convection flow through parallel-plates microchannel. Naterer [13] studied micro-fluidic fraction and thermal energy exchange in non-polarized electromagnetic field. Arikoglu *et al.* [14] researched the effect of slip on entropy generation in a single rotating disk in MHD flow. The main achievement of their work is to allow the designer to use the second law of thermodynamic in order to perform effective calculations of rotating fluidic system. Kiyasatfar *et al.* [15] studied the effect of magnetic flux density and applied current on entropy generation distributions in MHD pumps.

It should be noted here that in analyzing micropumps, in addition to velocity and volumetric flow rate, the heat generation and temperature distribution or generally the rate of entropy generation can also affect the efficiency of the system, and should be taken into account for a comprehensive study. Heat production and increase of temperature cause some limitations in special applications. This is why only few works have been dedicated to study of energy and entropy. Then the aim of this research is to investigate the effect of influencing parameters on heat production, velocity and temperature distributions and thus the rate of entropy production in MHD pumps.

Analyses and formulation of model

In the MHD micropump, the pumping forces are generated by the electromagnetic Lorentz force from applied electric currents. The basic principle relies on application of electric current across the channel filled with electrically conducting liquid and a DC magnetic field of permanent magnet that is in orthogonal direction to currents. A schematic view of the MHD pump and the coordinate set are illustrated in fig. 1.

The governing equations of the Lorentz force are derived based on this assumption that steady-state fields with constant magnetic and electric properties exist in working fluid. Hence, Ohm's law and Lorentz force can be written as:

$$\vec{J} = \sigma(\vec{E} + \vec{V} \times \vec{B}) \quad (1)$$

$$\vec{F} = \vec{J} \vec{B} \quad (2)$$

While the Reynolds number in micro-channel is assumed to be small, the flow field in the MHD micro-pump is treated as steady-state, incompressible, and fully developed laminar flow condition. Since dimensions of the channel in y- and z-directions are much smaller than in flow direction, the flow velocities in y- and z-directions are assumed to be zero. The effect of surface tension is neglected because the microchannel is assumed to be filled with fluids. Based upon the above assumptions, the axial flow velocity $u(y, z)$ is invariant along x-direction. For the simplified flow field, the governing equations can be written as:

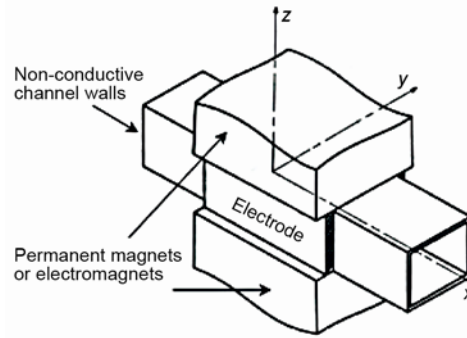


Figure 1. Schematic drawing of MHD pump

– continuity equation

$$\frac{\partial u}{\partial x} = 0 \quad (3)$$

– momentum equations

$$0 = -\frac{\partial p}{\partial x} + \mu \left(\frac{\partial^2 u}{\partial y^2} + \frac{\partial^2 u}{\partial z^2} \right) \quad (4)$$

$$-\frac{\partial p}{\partial y} = -\frac{\partial p}{\partial z} = 0$$

In the micro-channel under electromagnetic interactions, the Lorentz forces acting on the fluid particles are considered as a hydrostatic pressure head uniformly distributed over the entire channel region; hence, it is expressed as follows:

$$-\frac{\partial p}{\partial x} = \frac{\Delta p}{L} \quad (5)$$

where ΔP is the pressure head along the channel with length L , caused by interaction between magnetic and electric fields. That is:

$$\Delta p = (\vec{J} \times \vec{B})L_p - p_l \quad (6)$$

From eqs. (2), (5), and (6), the pressure gradient generated by the applied DC electric and magnetic fields in the flow channel can be obtained. After the pressure gradient is substituted into eq. (4), the momentum equation can be rewritten as:

$$0 = \frac{1}{\mu L} (\sigma B E l_p - \sigma B^2 u l_p - p_l) + \frac{\partial^2 u}{\partial y^2} + \frac{\partial^2 u}{\partial z^2} \quad (7)$$

Hence, the volumetric flow rate (Q) based upon the integral of cross-sectional channel area is given by:

$$Q = \iint u(y, z) dy dz \quad (8)$$

– energy equations

$$\rho c_p \left(\frac{DT}{Dt} \right) = k \nabla^2 T + \mu (\nabla u)^2 + \frac{J \cdot J}{\sigma} \quad (9)$$

With respect to the above assumptions the energy equation will be:

$$0 = k \left[\left(\frac{\partial^2 T}{\partial^2 y} \right)^2 + \left(\frac{\partial^2 T}{\partial^2 z} \right)^2 \right] + \mu (\nabla u)^2 + \frac{J \cdot J}{\sigma} \quad (10)$$

The boundary conditions for solving the governing equations are:

- In all boundaries the no-slip boundary condition is: $u(y, z) = 0$.
- The electrode and magnets are assumed to be in room temperature (25 °C).

For solving the non-linear differential equations, the code upon finite difference method is developed and utilized.

Entropy generation equations

The volumetric rate of local entropy generation can be expressed in the form:

$$S_{\text{gen}}^m = (S_{\text{gen}}^m)_{\text{heat}} + (S_{\text{gen}}^m)_{\text{fric}} + (S_{\text{gen}}^m)_{\text{magnetic effect}} \quad (11)$$

$$(S_{\text{gen}}^m)_{\text{heat}} = \frac{k}{T^2} \left[\left(\frac{\partial T}{\partial y} \right)^2 + \left(\frac{\partial T}{\partial z} \right)^2 \right] \quad (12)$$

$$(S_{\text{gen}}^m)_{\text{fric}} = \frac{\mu}{T} \left[\left(\frac{\partial u}{\partial y} \right)^2 + \left(\frac{\partial u}{\partial z} \right)^2 \right] \quad (13)$$

$$(S_{\text{gen}}^m)_{\text{magnetic effect}} = \frac{1}{T} \frac{J^2}{\sigma} \quad (14)$$

The total entropy generation rate over the volume (S_{gen}^t) can be calculated:

$$S_{\text{gen}}^t = \oint S_{\text{gen}}^m dV \quad (15)$$

Results and discussion

Considering this fact that the velocity and temperature distributions are affected not only by applied conditions but also by physical properties of working fluid and in order to generalize of the results, two electrical conductive fluids, namely, PBS solution and liquidous gallium are employed as working mediums for numerically simulating the DC MHD pump. These fluids are chosen because of their great differences in electrical and thermal conductivity. The related material properties of PBS solution and liquid gallium are summarized in tab. 1. In addition, the geometric dimensions and applied field's rates for simulations are listed in tab. 2.

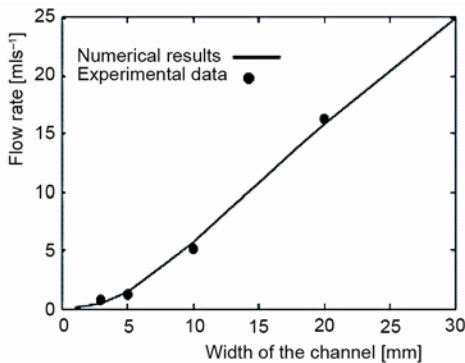
Table 1. Material properties of PBS solution and gallium

	Density	Electric conductivity	Dynamic viscosity	Thermal conductivity	Relative permeability	Relative permittivity
PBS solution	1058	1.5	0.0006	0.596	1	72
Gallium	5910	$7.30 \cdot 10^6$	$1.89 \cdot 10^{-3}$	40.6	1	-

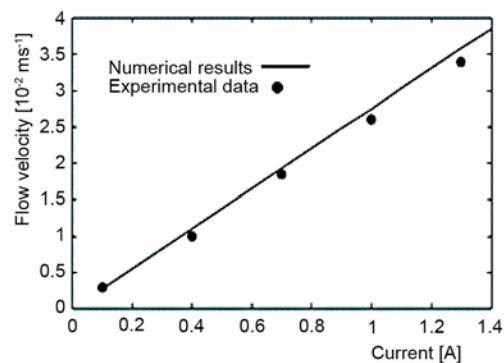
The numerical model is first compared with experimental data [8]. Figure 2 shows the numerical and experimental results for the volumetric flow rate as a function of the channel's width as well as mean flow velocity behaviors with change in applied current. According to fig. 2(b), as applied current increases, the numerical solutions begin to deviate from the experimental results. This is because of bubbles' growth in aqueous solutions caused by increasing in applied current that consequently affects the flow motion.

Table 2. Parameters for numerical simulation

Parameter	Value
Channel depth, [m]	0.007
Channel width, [m]	0.003
Channel length, [m]	0.08
Electrode length, [m]	0.035
Magnetic flux density, B [T]	0.008 ~ 0.4
Input current, I [A]	0.1 ~ 1.4



(a) PBS solution, $I = 0.7$ A, $B = 0.02$ T



(b) PBS solution, $B = 0.02$ T

Figure 2. Comparison between numerical results and experimental data

Flow velocity and temperature predictions

Figure 3 shows the maximum velocity of PBS solution as functions of various applied electric currents and magnetic flux density.

As it is clear from fig. 3, in PBS solution by increasing in applied electric current for a constant magnetic flux density, or by increasing in magnetic flux for a constant electric current, the maximum velocity linearly increased. Then it can be inferred that the flow rate can be increased in order to enhance the performance of the pump for a low electrically conductive fluids. This is applicable if the magnitude of applied current or the magnetic fields are able to be increased.

The same result is obtained for Gallium when electric current is increasing by keeping constant the magnetic flux density, fig. 4(a). However, according to fig. 4(b), the gallium velocity does not increase linearly with the magnetic flux density and has a peak. This show that the reverse Lorentz forces resulted by fluid flow in interaction with magnetic field, is sig-

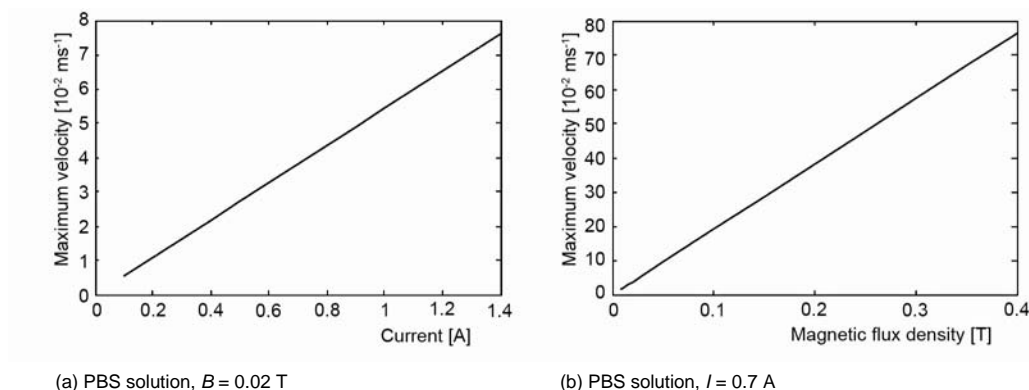


Figure 3. Maximum velocity of PBS solution as functions of various applied currents and magnetic field density

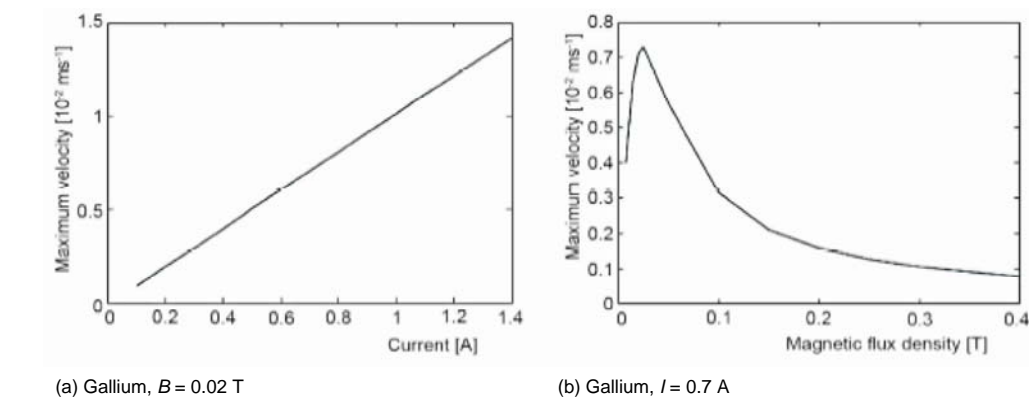


Figure 4. Maximum velocity of gallium as functions of various applied currents and magnetic field density

nificantly hampering the flow of fluid. The reason of different behavior of these two fluids is that the electric conductivity of PBS solution is far smaller than the conductivity of gallium (about 10^6). It is obvious from eq. (1), that the induced current in PBS solution is drastically low compared with the value of induced current in Gallium. Therefore, the maximum velocity and corresponding flow rate of PBS solution increases linearly with the applied current and magnetic field without being affected by the induced reverse Lorentz forces. According to fig. 5, by increasing in magnetic field, the reverse Lorentz force due to interaction between induced electric current and magnetic field is increasing. It should be noted that this phenomena is more crucial for fluids with high electrical conductivity.

Therefore, when using liquid metals as a working medium in MHD pumps, the reverse induced Lorentz forces are significant and the peak velocity occurs in a specific value of magnetic flux density. In fact, for higher Hartman numbers the velocity profiles within micro channel are going to be flatter and the maximum velocity is getting low, fig. 6(a).

Figures 7 and 8 show the maximum temperatures inside the channel as a function of electric current and magnetic flux for two types of working medium. According to fig. 7, the electric current notably affects the temperature of the PBS solution inside the channel. Whereas, the maximum temperature increases exponentially by increasing in applied electric current. But the intensity of magnetic field has a negligible effect on the temperature.

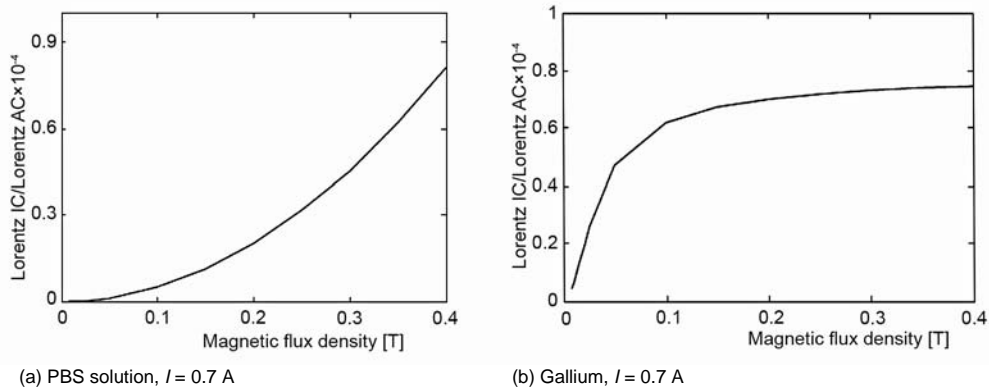


Figure 5. Ratio of Lorentz forces generated by the interactions between the induced currents (IC) and the magnetic field to Lorentz forces given by the applied currents (AC)

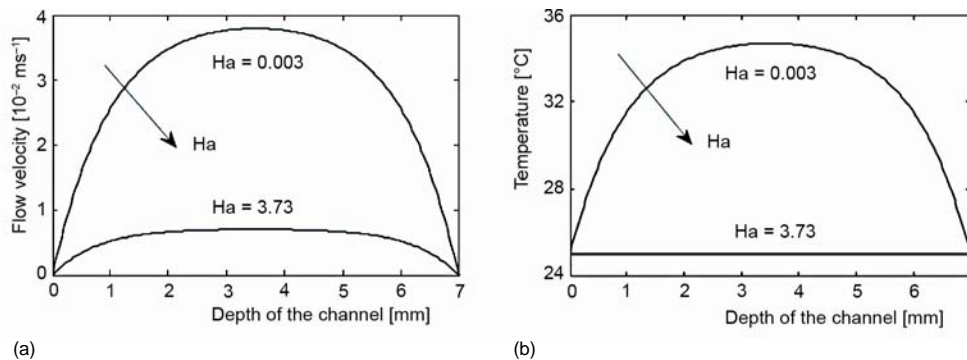


Figure 6. Variation of the mid width velocity and temperature with the depth of channel at different Hartman numbers

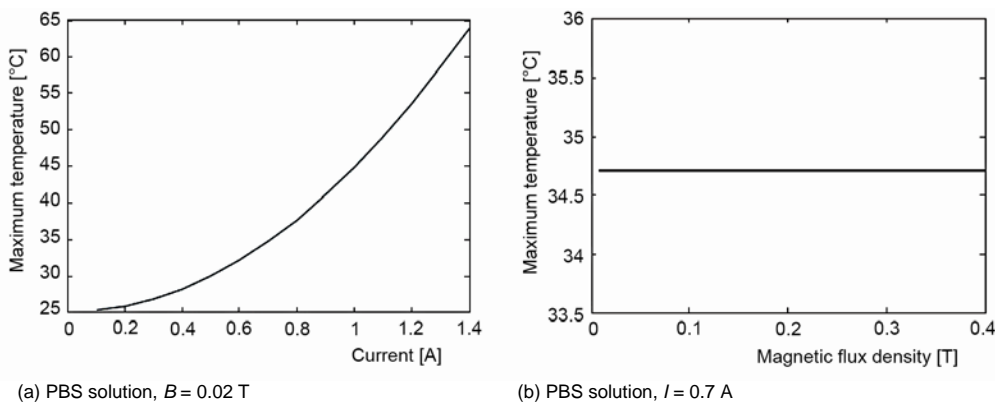


Figure 7. Maximum temperature in PBS solution as functions of various applied currents and magnetic field density

Figure 8 implies that the magnetic flux and electric current has not considerable effect on Gallium temperature, where it remains in its initial state. The main rationale is that the electric conductivity of gallium is high and as a consequence its electrical resistance will be low. Therefore, the generated heat inside the channel from interaction between electromagnetic

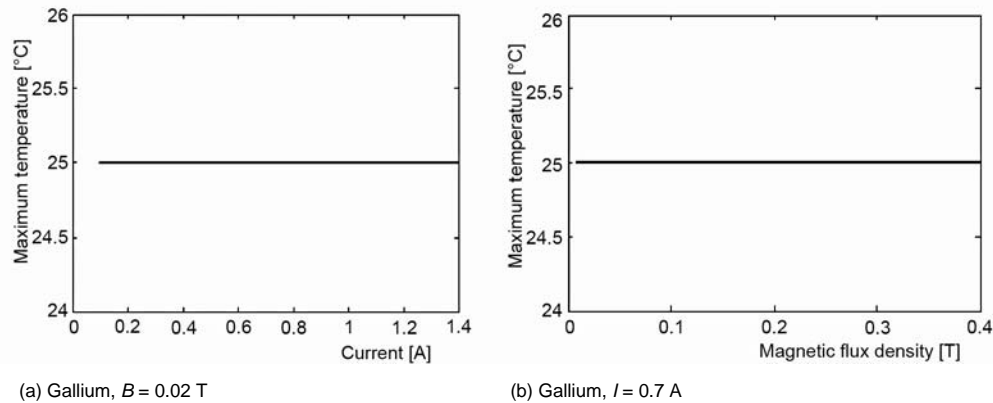


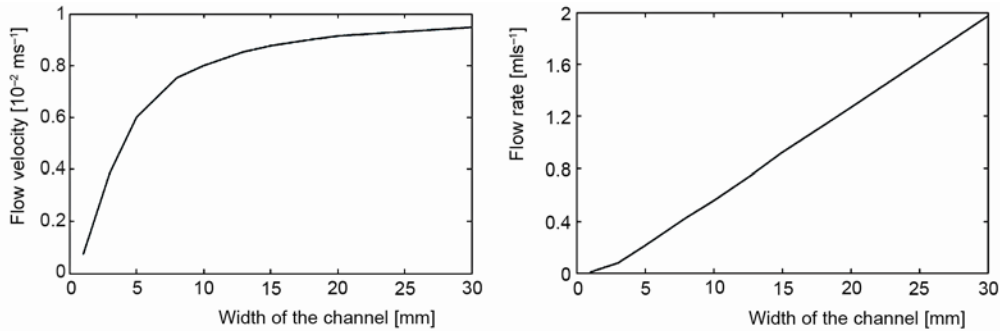
Figure 8. Maximum temperature in gallium as functions of various applied currents and magnetic field density

fields and the electric current in the working medium will be limited. On the other hand, relatively high thermal conductivity of the gallium possesses the ability to transfer generated heat to environment. The overall results of analyzing figs. 7 and 8, show that Ha number has a direct effect on temperature profile similarly to velocity profile. It is seen that at low Hartman number the temperature profiles are parabolic, and as Ha increases, the profiles gradually flatten and tends to be uniform, fig. 6(b). This means that, the electrical conductivity and viscosity can be used as a tool for controlling the velocity and the temperature.

Effects of channel geometry

Channel geometry has a direct effect on parameters such as the value of effective forces in velocity profiles, desired current density passing through the fluid and the value of generated heat inside the channel. Considering them, in this section, the effects of cross-sectional geometry of the channel on velocity and temperature distributions are investigated. Figure 9(a), depict the flow velocity of gallium as a function of width of the channel. According to the fig. 9(a), the flow velocity drastically reduced because of the resistance of frictional effect of the channel sidewalls when the width is less than a given size that is relevant to properties of working medium and applied conditions. In addition, the frictional forces between the fluid and the sidewalls of the channel are reducing as the channel width increases. Figure 9(b), shows the dependence of volumetric flow rate to channel width. It is seen that the flow rate increases linearly with the channel width. Also the same results are obtained by change in working medium to PBS solution. Velocity and flow rate of PBS solution are offered in fig. 10 as a function of channel's depth. It is obvious that the flow velocity is significantly reducing by reduction in the depth of channel. This is because of the frictional effect of the upper and lower channel walls. Also by increasing in the depth of channel, the reduction in the flow velocity is observed because of the reduction in applied current density passing through the fluid. Figure 10(b), depicts that the volumetric flow rate typically increases with the channel depth almost proportionally.

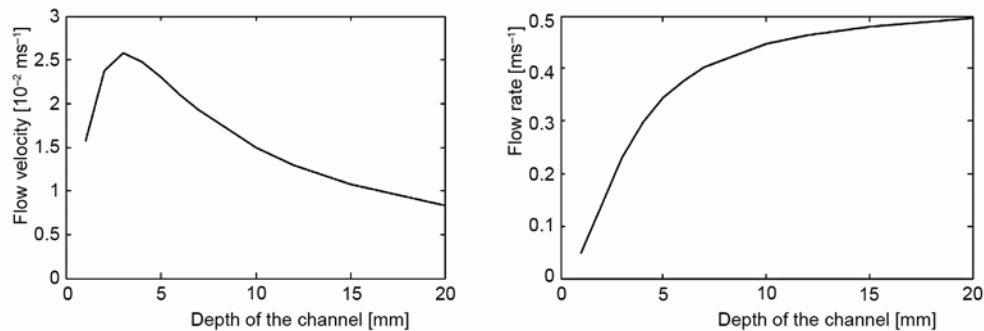
Similar to the prediction shown in fig. 10(a), the flow rate also exhibits a maximum along with the gradual increases in depth. The same behaviors are seen by using the gallium as a working medium. Therefore, an optimal depth of the channel can be determined according to the given geometry and operation conditions.



(a) Gallium, $I = 0.7 \text{ A}$, $B = 0.02 \text{ T}$

(b) Gallium, $I = 0.7 \text{ A}$, $B = 0.02 \text{ T}$

Figure 9. Velocity and flow rate of gallium as a function of width of the channel; $d = 7 \text{ mm}$

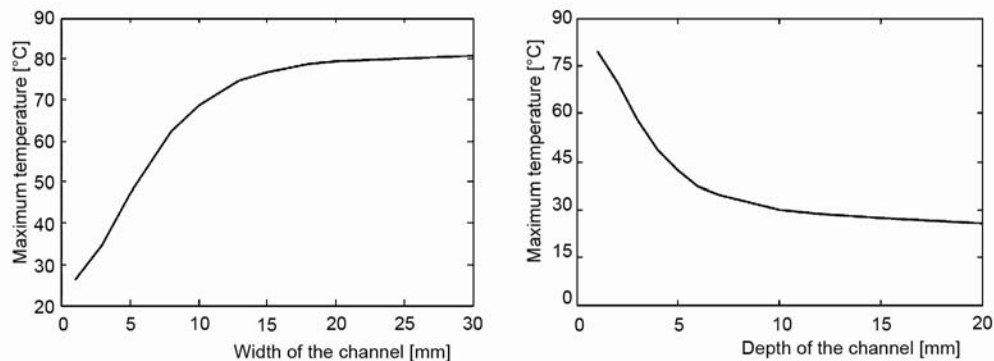


(a) PBS solution, $I = 0.7 \text{ A}$, $B = 0.02 \text{ T}$

(b) PBS solution, $I = 0.7 \text{ A}$, $B = 0.02 \text{ T}$

Figure 10. Velocity and flow rate as a function of depth of the channel; $w = 3 \text{ mm}$

The dependence of maximum temperature of the PBS solution to cross section of the channel is illustrated in fig. 11. As it can be seen, the maximum temperature is increased by increase in width of the channel. This is because of the electrical resistant along with channel width. Also the maximum temperature is decreased with increase in depth of the channel. This is because of the diminution of heat generation inside of the channel in consequence of decreasing in applied current density. These behaviors are happening in the given dimensional spans.



(a) PBS solution, $I = 0.7 \text{ A}$, $B = 0.02 \text{ T}$, $d = 7 \text{ mm}$

(b) PBS solution, $I = 0.7 \text{ A}$, $B = 0.02 \text{ T}$, $w = 3 \text{ mm}$

Figure 11. Maximum temperature as functions of width and depth of the channel

With further increment in width and depth, the effect of channel cross-section on the maximum temperature is dwindle. These specific dimensional spans are related to the applied conditions and properties of the working medium. By employing liquid gallium as a working medium, through high electrical and thermal conductivity, the variations of the width and depth of the channel no longer affect the maximum temperature.

Entropy generation rate

The velocity, temperature, and electric current density fields were discussed. In this section, the entropy generation rate within the MHD channel will be determined. Mean volumetric local entropy generation rates in MHD flow inside the channel as functions of various applied currents and magnetic flux density are shown in figs. 12 and 13.

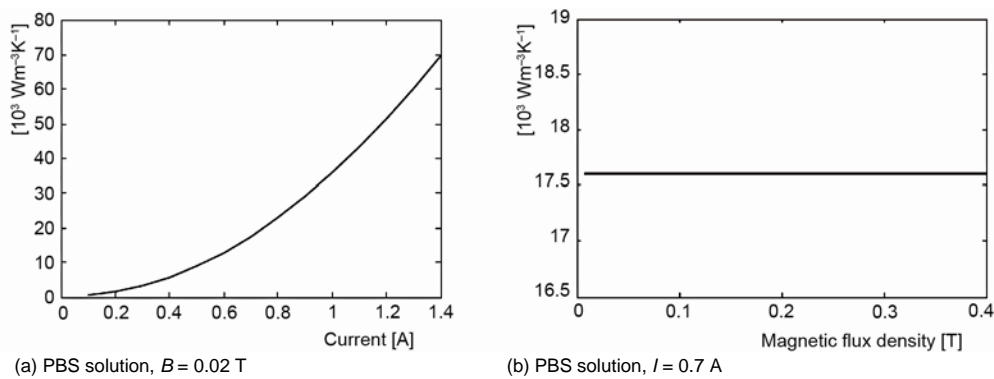


Figure 12. Mean local volumetric entropy generation rate in PBS solution as functions of various applied currents and magnetic field intensity

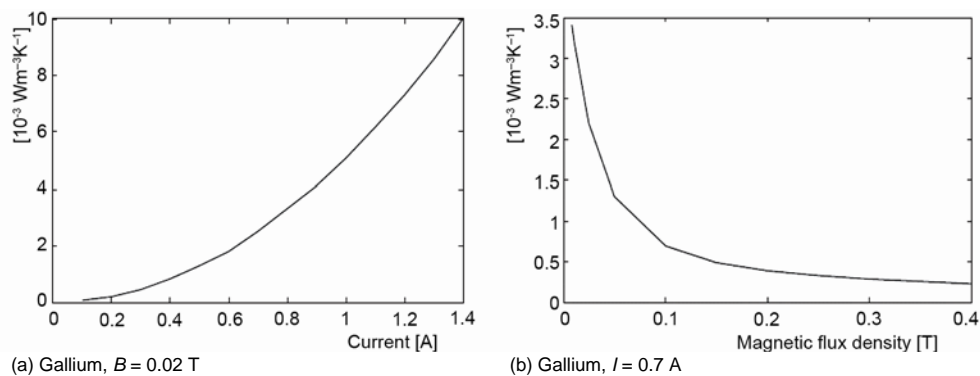


Figure 13. Mean local volumetric entropy generation rate in gallium as functions of various applied currents and magnetic field density

According to fig. 12, with the use of low electrically and thermally conductive fluid such as PBS solution in MHD pumps, the mean local volumetric entropy generation rate increases exponentially by increasing in applied electric current and remains roughly constant with change in magnetic flux density. It is apparent from fig. 13 that when high electrically and thermal conductive fluid (such as gallium) are employed as a working medium, with increasing in electric current, the entropy generation rate in MHD pumps behave similar to PBS solution and show notably descent by increasing in magnetic field intensity.

It has been shown that the entropy generation rate can be minimized under different conditions that involve specific relations of physical properties of the fluid, a particular geometry, or given operation conditions of the channel. Minimization of the entropy generation rate can be used as a design tool in micro fluidic applications particularly in MHD pumps.

Conclusions

From the results and analysis of the present numerical simulation, following conclusions can be obtained:

- In the low electrical conductive fluid as a PBS solution, by increasing in the magnetic flux density or in the applied electric current, the maximum velocity increased linearly.
- In the high electrical conductive fluid as a liquid gallium, by increasing in the magnetic flux density, the maximum velocity does not increase linearly and have a peak.
- When using liquid metals as a working medium in MHD pumps, the reverse induced Lorentz forces are significant and the peak velocity is happening in a specific value of magnetic flux density.
- At small Hartman numbers, the velocity and temperature profiles are parabolic. Increases in Ha number are lead to decrease in velocity and temperature and so their profiles get flat.
- Electric current notably affects the temperature of the low electrical conductive fluid inside of channel. Whereas, the maximum temperature increases exponentially by increasing in applied electric current. But the intensity of magnetic field has a negligible effect on the temperature.
- Cross-sectional channel geometry because of determinant effect on the frictional forces and value of current density passing through the fluid, has a direct effect on the velocity and temperature distributions inside the MHD channel. Therefore, an optimal cross sectional geometry of the channel can be determined according to the operation conditions and physical properties of working medium.
- The entropy generation rate inside the channel in MHD pumps can be minimized under different conditions that involve specific relations of physical properties of the fluid, a particular geometry, or given operation conditions of the channel.

Nomenclature

B	– magnetic flux density, [T]	Re	– Reynolds number, $(\rho u D / \mu)$
d	– depth of channel, [m]	S	– entropy generation rate, $[\text{Wm}^{-3}\text{K}^{-1}]$
E	– electric field intensity, $[\text{Vm}^{-1}]$	T	– temperature, [K]
F	– Lorentz forces, $[\text{Nm}^{-3}]$	u	– velocity components in the x- directions, $[\text{ms}^{-1}]$
Ha	– Hartman number, $[Bw(\sigma/\mu)^{-1/2}]$	w	– width of channel [m]
I	– electric current, [A]	<i>Greek symbols</i>	
J	– electric current density, $[\text{Am}^{-2}]$	δ	– liquid's conductivity, $[\text{Nsm}^{-2}]$
k	– thermal conductivity, $[\text{Wm}^{-1}\text{K}^{-1}]$	μ	– dynamic viscosity, $[\text{kgm}^{-1}\text{s}^{-1}]$
L	– length of channel, [m]	ρ	– density, $[\text{kgm}^{-3}]$
L_p	– length of electrode, [m]		
\dot{Q}	– volumetric flow rate, $[\text{m}^3\text{s}^{-1}]$		

References

- [1] Lemoff, A., *et al.*, An AC Magnetohydrodynamic Micropump. Towards a True Integrated Microfluidic System, International Conference on Solid-State Sensors and Actuators, *Transducers*, 99 (1999), 2, pp. 1126–1129
- [2] Lemoff, A, Lee, A., An AC Magnetohydrodynamic Micropump, *Sens. Actuators*, 63 (2000), 3, pp. 178-185

- [3] Jang, J., Lee, S. S., Theoretical and Experimental Study of MHD Micro-Pump, *Sens. Actuators*, 80 (2000), 6, pp. 84-89
- [4] Lemoff, A, Lee, A., An AC Magnetohydrodynamic Microfluidic Switch for Micro Total Analysis Systems, *Biomed Microdevices*, 5 (2003), 1, pp. 55-60
- [5] Wang, P.-J. et al., Simulation of Two-Dimensional Fully Developed Laminar Flow for a Magneto-Hydrodynamic (MHD) Pump, *Biosensors and Bioelectronics*, 20 (2004), 1, pp. 115-121
- [6] Homsy, et al, A High Current Density DC Magneto-Hydrodynamic (MHD) Micro-Pump, *The Royal Society of Chemistry, Lab Chip*, 5 (2005), 4, pp. 466-471
- [7] Duwairi, H. M., Abdullah, M., Thermal and Flow Analysis of a Magneto-hydrodynamic Micro-pump, *Micro-System Technologies*, 13 (2007), 1, pp. 33-39
- [8] Ho, J. E., Characteristic Study of MHD Pump with Channel in Rectangular Ducts, *Journal of Marine Science and Technology*, 15 (2007), 4, pp. 315-321
- [9] Bejan, A., Second Law Analysis in Heat Transfer, *Energy*, 5 (1980), 8-9, pp. 721-723
- [10] Bejan A., *Entropy Generation Minimization*, CRC Press, Boca Raton, Fla., USA, 1996
- [11] Salas, H, et al., Entropy Generation Analysis of Magnetohydrodynamic Induction Devices, *Journal of Physic D: Applied Physic*, 32 (1999), 20, pp. 2605-2608
- [12] Haddad, O, et al., Entropy Generation due to Laminar Incompressible Forced Convection Flow through Parallel-Plates Microchannel, *Entropy*, 6 (2004), 5, pp. 413-426
- [13] Naterer, G. F., Microfluidic Friction and Thermal Energy Exchange in a Nonpolarized Electromagnetic Field, *Int. J. Energy Res.*, 31 (2007), 6-7, pp. 728-741
- [14] Arikoglu, A., et al., Effect of Slip on Entropy Generation in a Single Rotating Disk in MHD Flow, *Applied Energy*, 85 (2008), 12, pp. 1225-1239
- [15] Kiyasatfar, M., et al, Effect of Magnetic Flux Density and Applied Current on Temperature, Velocity and Entropy Generation Distributions in MHD Pumps, *Sensors & Transducers Journal*, 124 (2011), 1, 72-82